Supplementary Information

Unlocking the Structure of Mixed Amorphous-Crystalline Ceramic Oxide Films Synthesized Under Low Temperature Electromagnetic Excitation

Nathan Nakamura[a], Maxwell W. Terban[b], Simon J. L. Billinge[b, c], and B. Reeja-Jayan[a]

[a] *Department of Mechanical Engineering, Carnegie Mellon University, Pittsburgh PA 15213*
[b] *Department of Applied Physics and Applied Mathematics, Columbia University, New York NY 10027*
[c] *Condensed Matter Physics and Materials Science Department, Brookhaven National Laboratory, Upton NY 11973*

S1. MWR-Assisted Thin Film Synthesis - Summary of Reaction Conditions

Table S1: MWR-assisted synthesis reaction conditions

	Temperature (°C)	Time (min)	Power (W)
1	140	15	10
2	140	15	20
3	140	15	40
4	140	30	10
5	140	30	20
6	140	30	40
7	140	60	10
8	140	60	20
9	140	60	40
10	150	15	10
11	150	15	20
12	150	15	40
13	150	30	10
14	150	30	20
15	150	30	40
16	150	60	10
17	150	60	20
18	150	60	40
19	160	15	10
20	160	15	20
21	160	15	40
22	160	30	10
23	160	30	20
24	160	30	40
25	160	60	10
26	160	60	20
27	160	60	40

Experimental conditions for MWR power input, reaction temperature, and reaction time are shown in Table S1. MWR power was varied from 10-40 W, reaction solution temperature was varied between 140, 150, and 160 °C, and reaction time was either 15, 30, or 60 min.

S2. Pair Distribution Function (PDF) Analysis

The experimental PDF, $G(r)$, is related to the atomic pair density $\rho(r)$, given by:

$$G(r) = 4\pi r(\rho(r) - \rho_0)$$

$$\rho(r) = \frac{1}{4\pi N r^2} \sum_i \sum_{j \neq i} \frac{b_i b_j}{\langle b \rangle^2} \delta(r - r_{ij})$$

where ρ_0 is the atomic number density of the material, N is the number of atoms in the material, b_i and b_j are the scattering factors of atoms i and j, respectively, $\langle b \rangle$ is the average scattering factor, r_{ij} is the distance between atoms i and j, and δ is the Dirac delta function.[1]

The presence of finite structural coherence or nanocrystallites in the samples tends to dampen the experimental PDF signal as a function of r related to both the size and shape of the coherently scattering domains.[2] In the models, we correct for this by applying an envelope function $f(r,d)$ assuming spherical domains with diameter d,[2, 3] as

$$G_{nano}(r, d) = f(r, d)G(r)$$

$$f(r, d) = \left[1 - \frac{3r}{2d} + \frac{1}{2}\left(\frac{r}{d}\right)^3\right] H(d - r)$$

where $H(r)$ is a step function with value 1 for r≤d and 0 beyond. This function could be independently applied to separate phases in the same model. Refinement of all parameters utilized least-squares optimization, where the quality of the fit was characterized by the residual function R_w defined by

$$R_w = \sqrt{\frac{\sum_{i=1}^{N} [G_{obs}(r_i) - G_{calc}(r_i; P)]^2}{\sum_{i=1}^{N} {G_{obs}}^2(r_i)}}$$

where G_{obs} is the experimental PDF, G_{calc} is the calculated PDF, and P is the set of refinable parameters used in the structure model. In our refinements, lower values of R_w correspond to a higher quality fit, or a better match between the experimental PDF data and the calculated PDF from the refined structure.

Table S2: PDF measurement standards and experimental PDF resolution fitting parameters from standard refinements

Experiment	Detector distance (mm)	Wavelength (Å)	Standard	Q_{damp} (Å^2)	Q_{broad} (Å^2)
MWR-films	200.30	0.18270	CeO_2	0.0452	0.0029
Furnace-films	201.9203	0.18351	CeO_2	0.0392	0.0111
Bulk TiO_2 crystals	205.4850	0.18351	Nickel	0.0383	0.0165

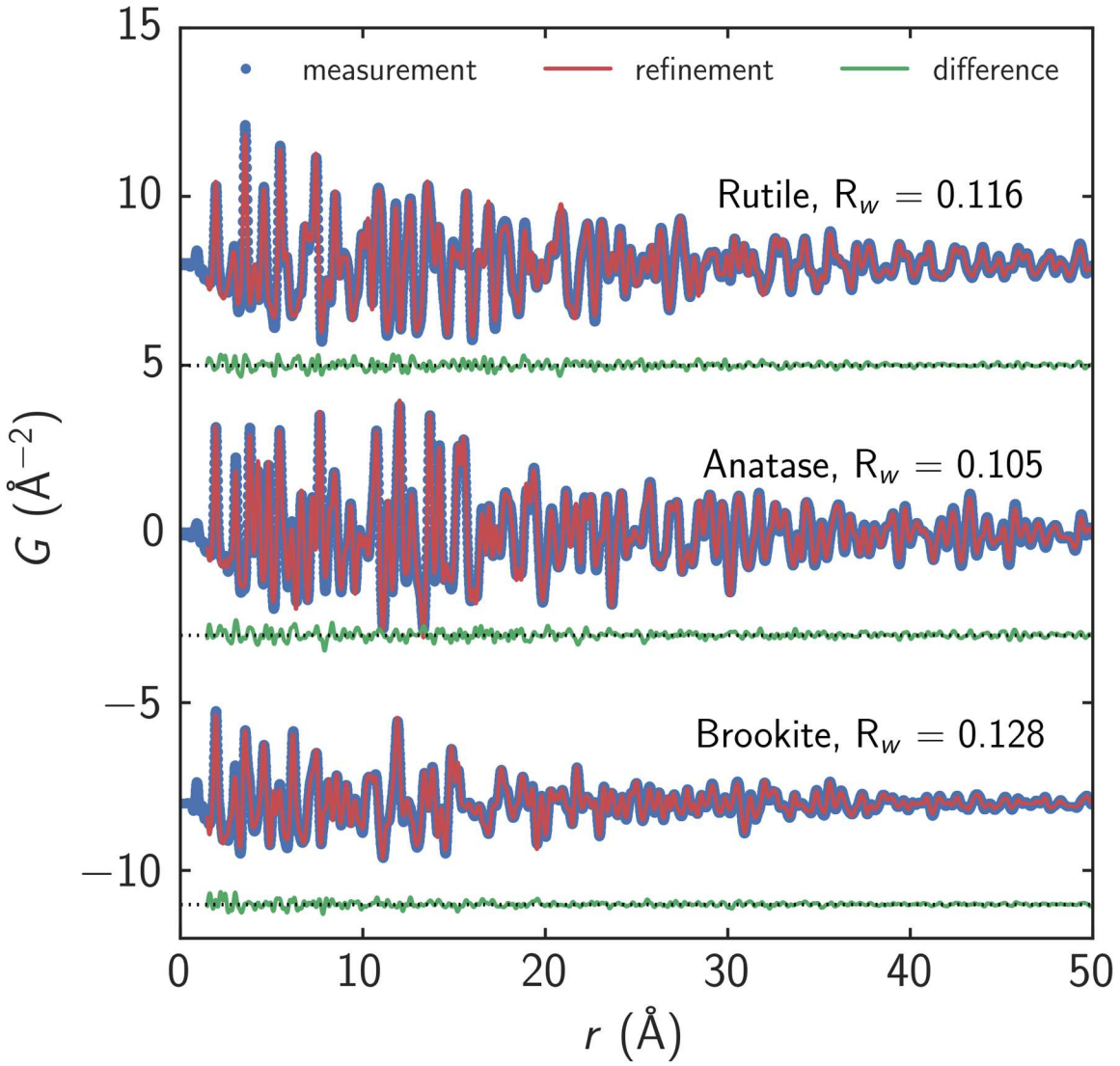

Fig. S1: Measured and refined PDFs shown for the three common TiO_2 forms: rutile, anatase, and brookite.

Table S3: Common form TiO_2 fit parameters

	Rutile	**Anatase**	**Brookite**
a (Å)	4.595	3.784	9.171
b (Å)	-	-	5.448
c (Å)	2.959	9.510	5.134
Ti U_{iso} (Å^2)	0.0062	0.0047	0.0047
O U_{iso} (Å^2)	0.0144	0.0117	0.0132
D_c (Å)	-	-	248
R_w	0.116	0.105	0.128

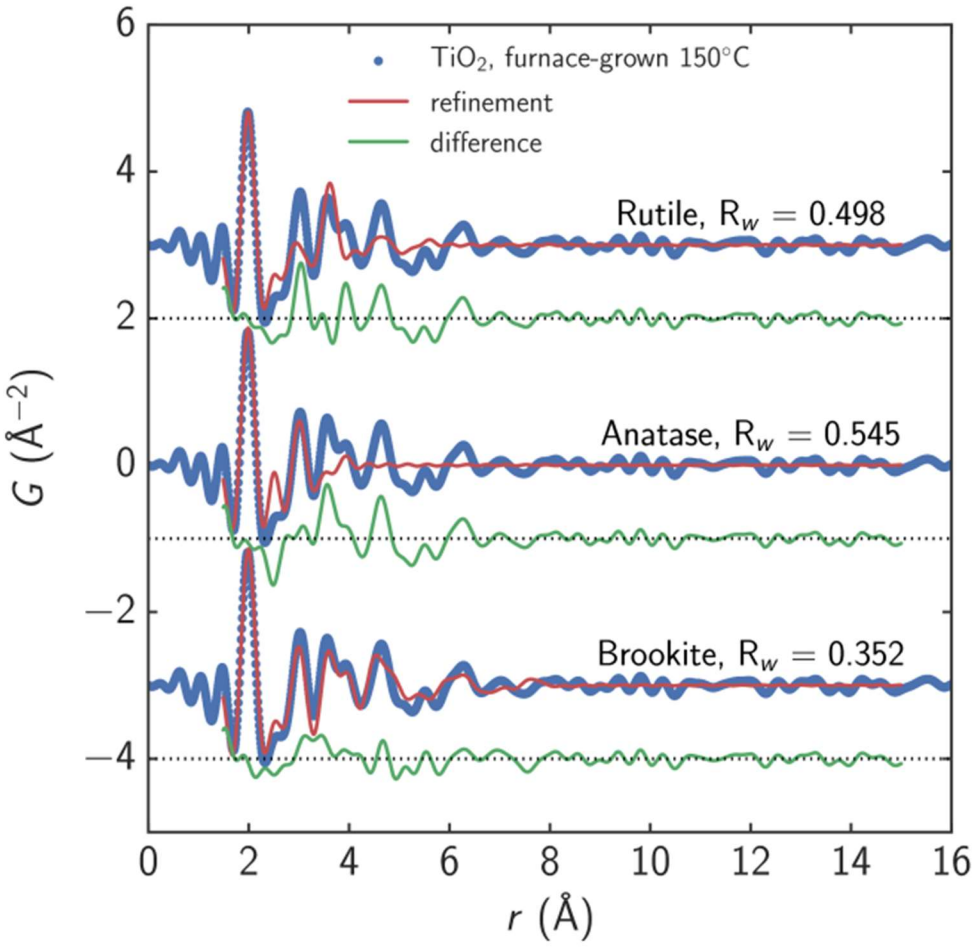

Fig. S2: Structural models for rutile, anatase, and brookite (red) fit to experimental PDF data (blue) from the 150°C furnace-grown film. Difference is shown offset below (green). Brookite provides the best single phase fit.

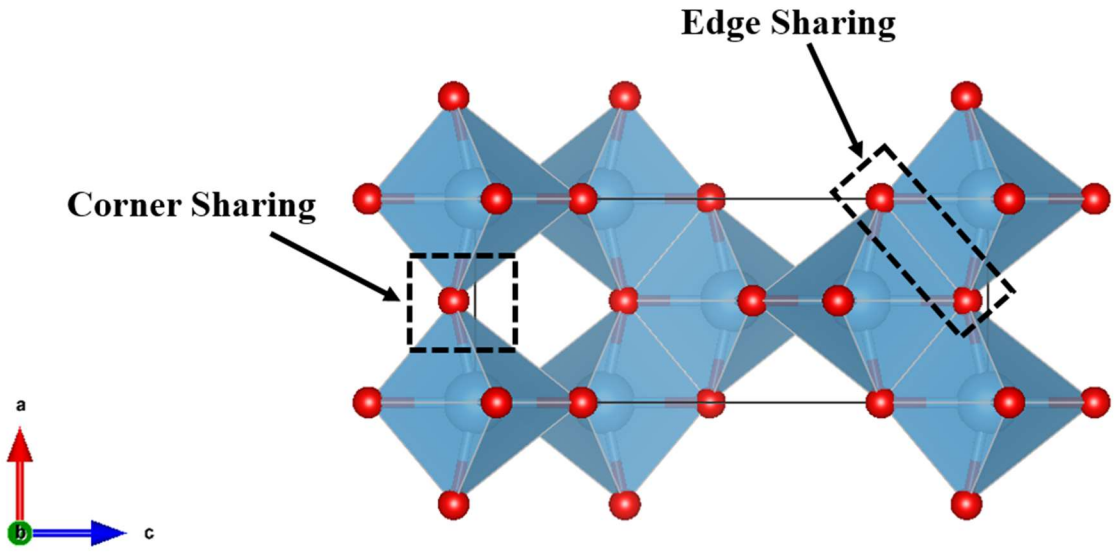

Fig. S3: Edge versus corner sharing in the anatase crystal structure. Corner sharing is present when two neighboring octahedrons share a single oxygen atom, while edge sharing corresponds to neighboring octahedrons sharing two adjacent oxygen atoms. Each octahedron in the anatase structure is neighbored by eight others, four of which are corner shared and four of which are edge shared.

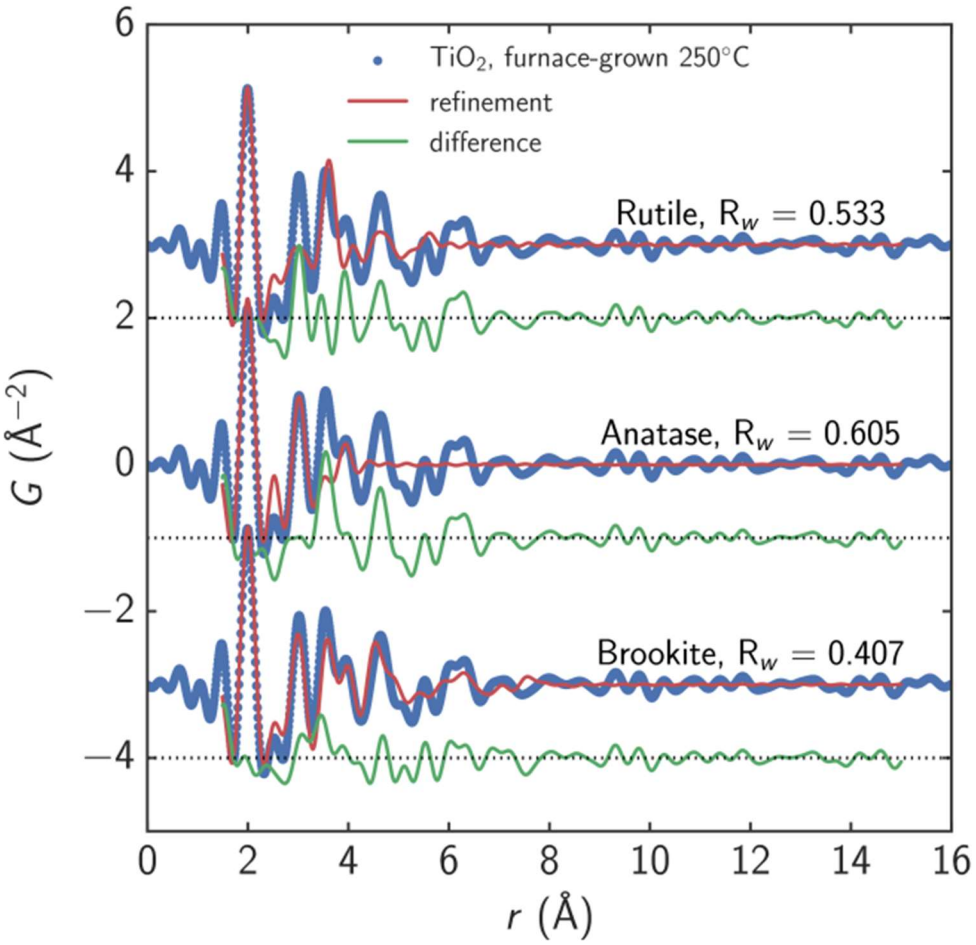

Fig. S4: Structural models for rutile, anatase, and brookite (red) fit to experimental PDF data (blue) from the 250°C furnace-grown film. Difference is shown offset below (green). No crystalline component was detected.

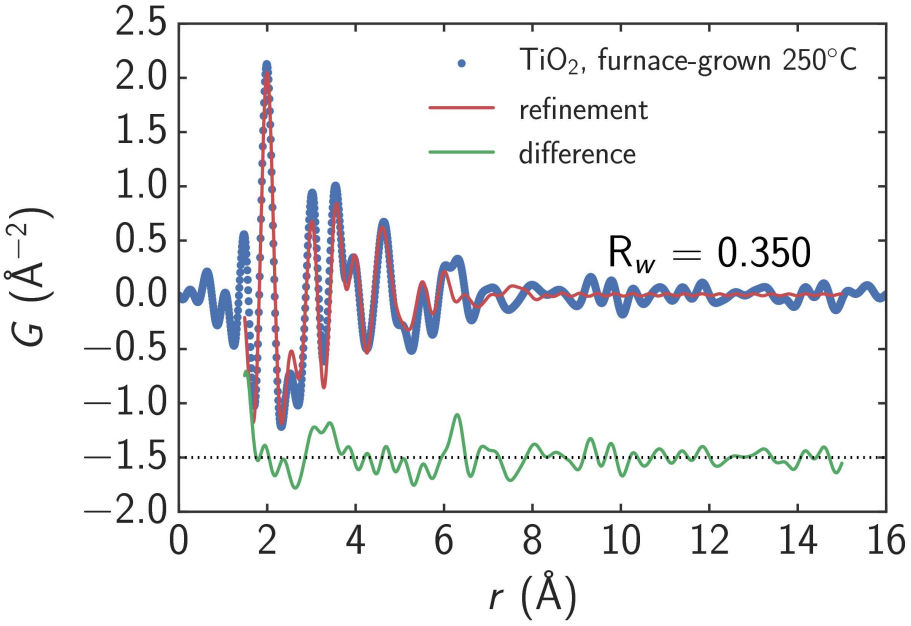

Fig. S5: Amorphous model (red) fit to experimental PDF data (blue) from the 250°C furnace-grown film. Difference is shown offset below (green). The brookite:anatase:rutile ratio was found to be 51:21:28.

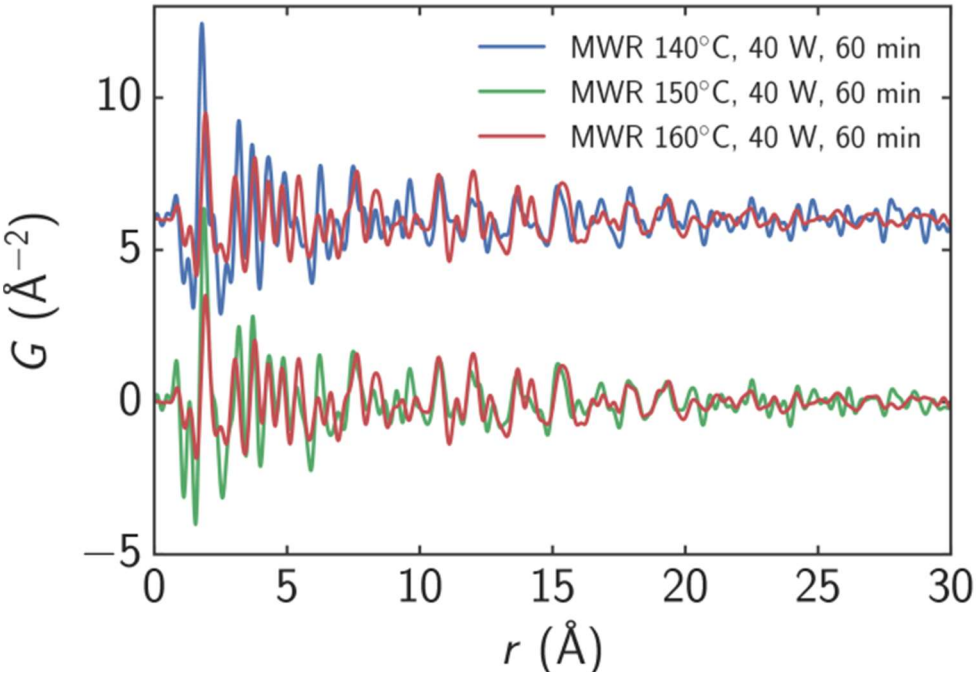

Fig. S6: Comparison of the PDFs for MWR-grown TiO_2 synthesized at 160°C (red) versus 140 (blue) and 150°C (green) at 40 W for 60 min. The signals in the MRO range are similar, indicating the presence of nanocrystalline anatase is consistent across MWR reaction conditions.

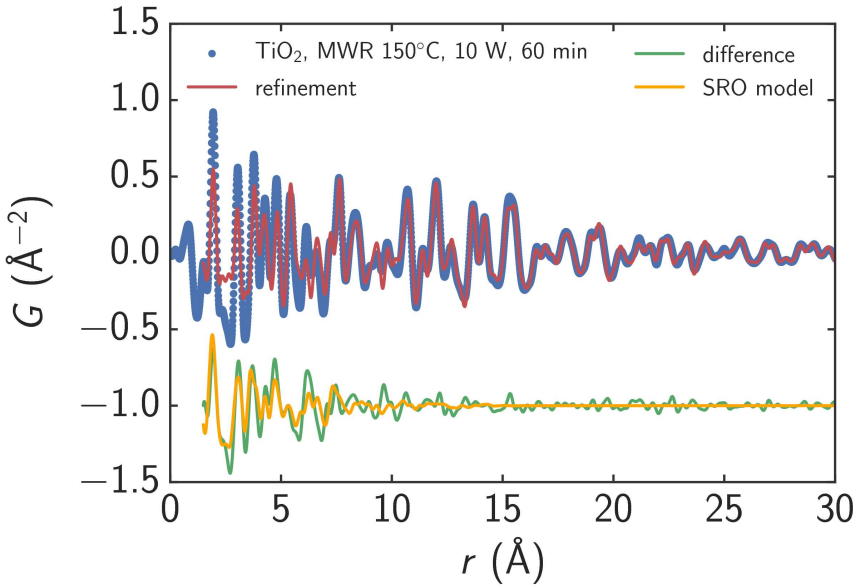

Fig. S7: MRO anatase model (red) fit to experimental PDF data (blue) from the powder sample scraped from a film grown using MWR at 150°C, 10 W, for 60 min. Difference is shown offset below (green), and the refined SRO model (orange) is superimposed for comparison.

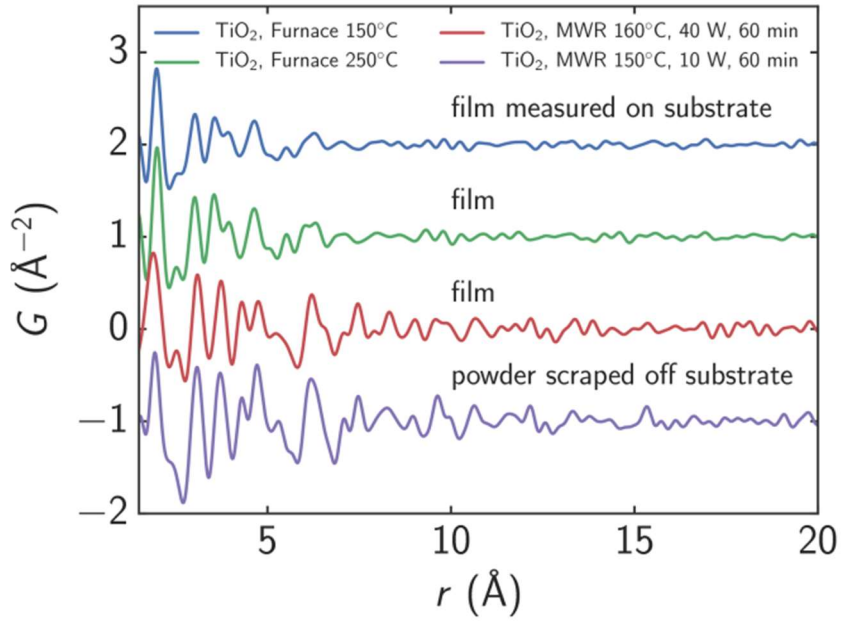

Fig. S8: Comparison of amorphous signals (SRO components) for furnace-grown and MWR-grown TiO_2 films. The amorphous signal from the MWR-grown films was isolated by fitting anatase to the long range structure and taking the difference. Comparison of MWR and furnace-grown amorphous components indicate clear difference in the SRO formed with and without EM field exposure. The furnace grown films were synthesized at 150°C and 250°C , and MWR-grown films were synthesized at 160°C, 40 W, 60 min and 150°C, 10 W, 60 min. The PDF data for the 150°C, 10 W, 60 min MWR-grown TiO_2 was acquired by scraping the film off the glass/ITO substrate and taking PDF data of the resultant powder. Pearson correlation coefficients for this PDF comparison are shown in Table S4.

Table S4: Pearson correlation coefficients for amorphous signals over a range of 1-20 Å. A value of 1 indicates perfect correlation, 0 indicates no correlation, and -1 indicates perfect anti-correlation. So, values close to 1 indicate that the structures are highly similar.

	Furnace 150°C	**Furnace 250°C**	**MWR 160°C**	**MWR 150°C**
Furnace 150°C	1.0	0.977	-0.201	-0.168
Furnace 250°C	-	1.0	-0.147	-0.122
MWR 160°C	-	-	1.0	0.908
MWR 150°C	-	-	-	1.0

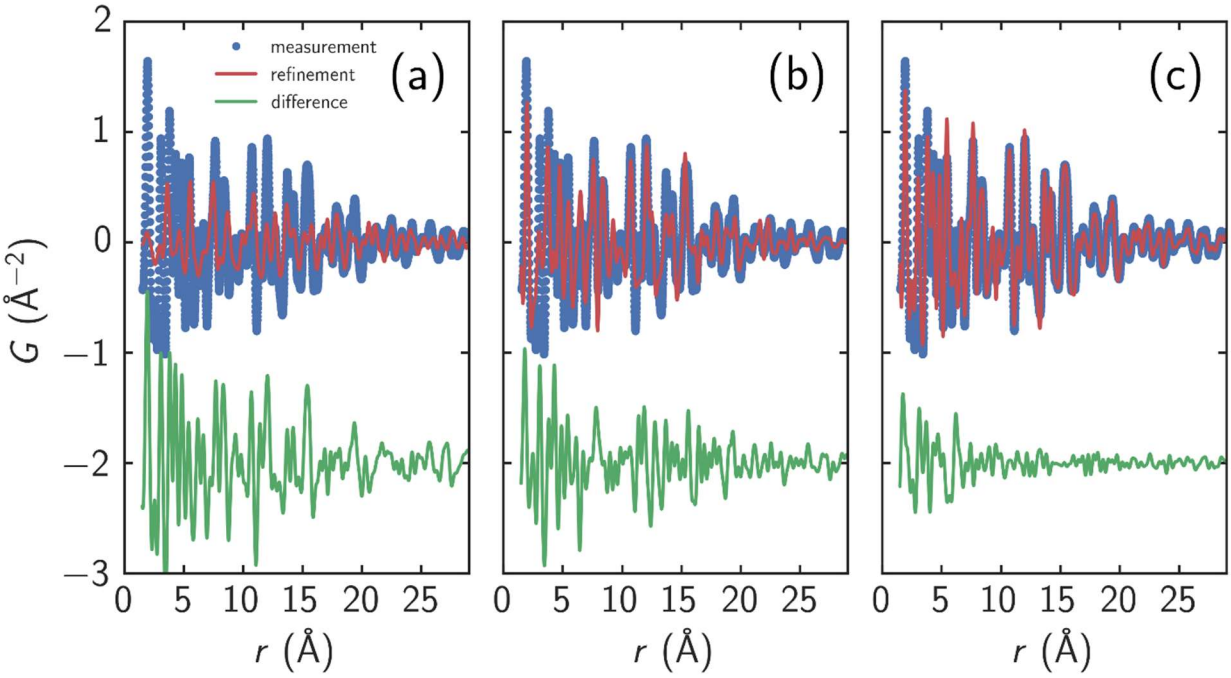

Fig. S9: Structural models for the three commonly occurring crystalline phases of TiO_2 (anatase, brookite, and rutile) were fit to the TiO_2 thin film PDF data. PDF fits of the single phase TiO_2 structures to the measurement for a 160 °C, 40 W, 60 min film using (a) rutile, (b) brookite, and (c) anatase. Anatase clearly outperforms the other structures.

Table S5: TiO_2 fit parameters for furnace/MWR films

	Furnace (450°C)	**Furnace (150°C)**	**Furnace (250°C)**	**MWR 150°C-10W-60min (scraped powder)**	**MWR 160°C-40W-60min**
MRO (anatase)					
a (Å)	3.790	-		3.785	3.789
c (Å)	9.500	-		9.497	9.501
Ti U_{iso} (Å^2)	0.0060	-		0.0064	0.0066
O U_{iso} (Å^2)	0.0196	-		0.0206	0.0209
D_c (Å)	106.2	-		68.2	55.3
δ_1	1.6376	-		1.29	0.82
SRO					
brookite:anatase:rutile	-	80:7:13	69:11:20	70:30:0	77:23:0
a (Å) (anatase)	-	3.539	3.381	3.869	3.886
c (Å) (anatase)	-	9.844	10.119	9.160	9.086
a (Å) (rutile)	-	4.364	4.563	-	-
c (Å) (rutile)	-	3.059	3.071	-	-
a (Å) (brookite)	-	9.720	9.764	9.089	9.193
b (Å) (brookite)	-	5.896	5.934	4.696	4.703
c (Å) (brookite)	-	4.905	4.805	5.524	5.508
Ti U_{iso} (Å^2)	-	0.0097	0.0035	0.0071	0.0051
O U_{iso} (Å^2)	-	0.0095	0.0047	0.0339	0.0304
D_c (Å)	-	10.6	9.4	16.5	11.8
δ_1	-	1.88	1.85	1.29	0.8186
Total					
MRO (%)	1.0	0.0	0.0	0.34	0.36
R_w	0.208	0.318	0.350	0.294	0.224

S3. Photon Energy Calculations from UV-Visible Spectra

The energy of the incident light during UV-visible spectra collection was found using the equation:

$$h_v = \frac{h * c}{\lambda}$$

Where h_v is the photon energy, h is the Planck constant ($4.135*10^{-15}$ eV*s), c is the speed of light ($3*10^8$ m/s), and λ is the wavelength of the incident light.

S4. Scanning Electron Microscopy (SEM) Results

Scanning electron microscopy (SEM) images were recorded using a Philips XL-30 FEG SEM operating in secondary electron mode with an incident energy of 15 kV and a spot size of 3. TiO_2 films grown by MWR-assisted synthesis display different surface morphology when compared to furnace-grown samples, as well as significantly smaller surface features and thicknesses (Fig. S10a-b). At higher magnification, it is clear that the surface of MWR-grown TiO_2 consists of conjoined spherical particles, whereas the surface of the larger furnace-grown blocks are relatively smooth (Fig. S11a-b). The shape and size of these features remained consistent across the film surface, but MWR-grown films experience significant variations in film thickness across the substrate. This is likely due to the edge effect phenomena, which leads to an increase in MWR absorption close to the edge of a conducting layer.[4] This non-uniform energy absorption subsequently leads to spatial heterogeneity in the thickness of MWR-grown films, with thicker films growing along the edges of the substrate and less material growing at the center.

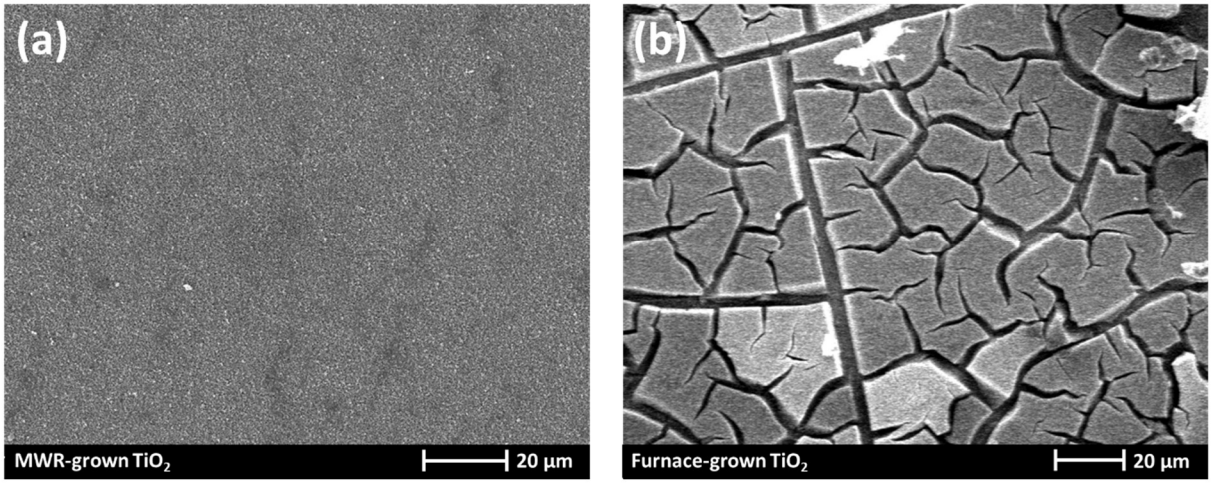

Fig. S10: (a) Surface of MWR-grown TiO_2 film synthesized at 140°C, 10 W constant power, and a 15 min hold time. (b) Surface of furnace grown film at 450°C. Magnification is 20 µm.

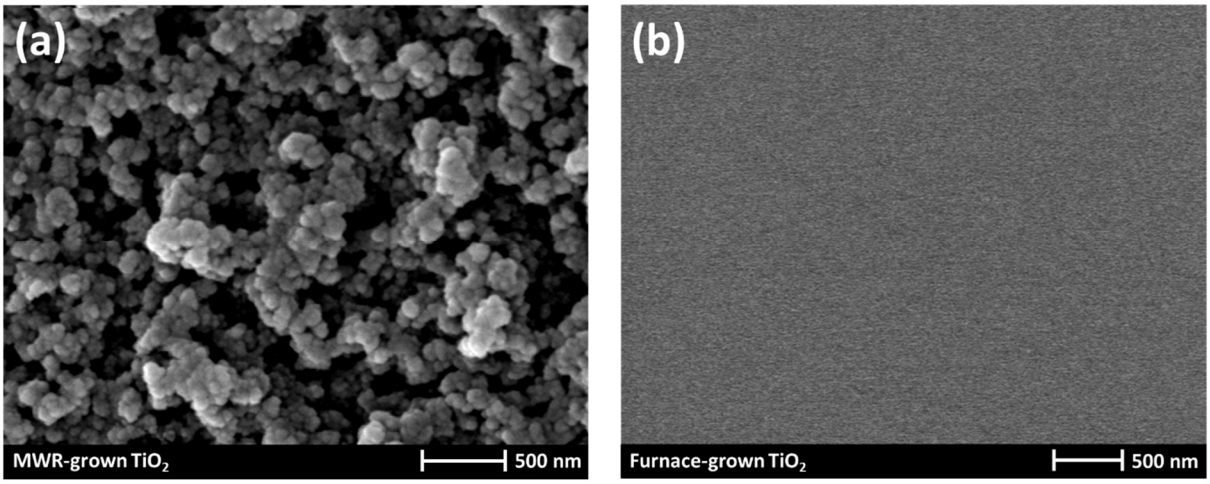

Fig. S11: (a) Surface of MWR-grown TiO_2 film synthesized at 140°C, 10 W constant power, and a 15 min hold time. (b) Surface of furnace grown film at 450°C. Magnification is 500 nm.

Cross-sectional SEM imaging was utilized to verify thickness measurements for MWR-grown films (Fig. S12a). MWR-grown films were found to vary in thickness from 450 to 1500 nm, while furnace-grown films were ~300 nm thick (Fig. S12b).

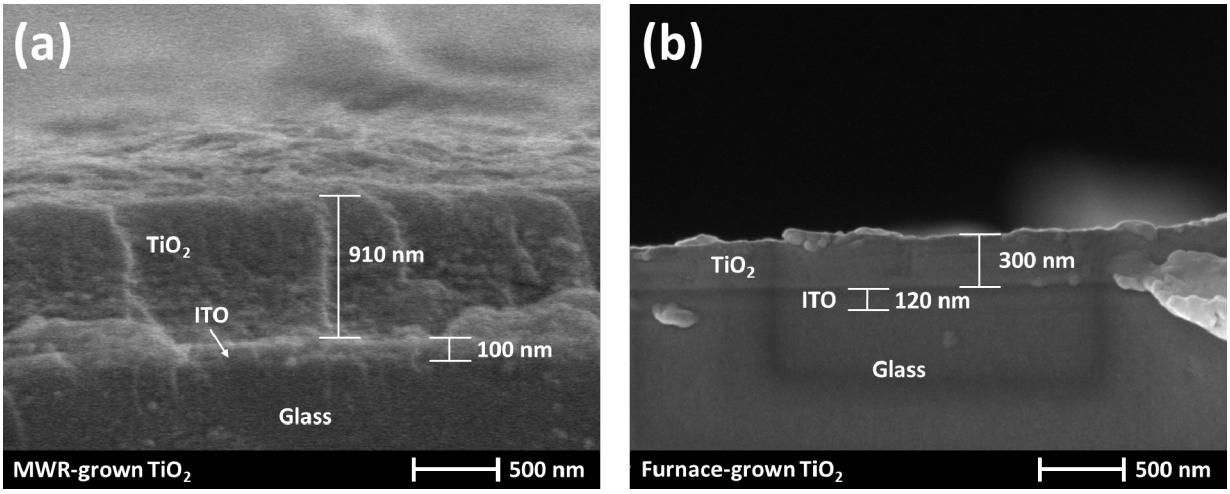

Fig. S12: (a) Cross-section of MWR-grown TiO_2 synthesized at 140°C, 10 W, and a 15 min hold. (b) Cross-section of TiO_2 film grown in the furnace at 450°C.

References

1. T. Egami and S. J. L. Billinge, *Underneath the Bragg Peaks: Structural Analysis of Complex Materials*, Elsevier, 2012.
2. K. Kodama, S. Iikubo, T. Taguchi and S. Shamoto, *Acta Cryst.*, 2006, **A62**, 444-453.
3. A. Guinier and G. Fournet, *Small-Angle Scattering of X-Rays*, John Wiley & Sons, Inc., New York, 1955.
4. J. Meixner, *IEEE Transactions on Antennas and Propagation*, 1972, **20**, 442-446.